NASA/TP-1998-206270

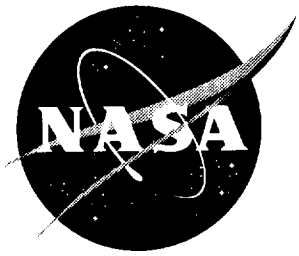

Modeling the Benchmark Active Control Technology Wind-Tunnel Model for Active Control Design Applications

Martin R. Waszak
Langley Research Center, Hampton, Virginia

National Aeronautics and
Space Administration

Langley Research Center
Hampton, Virginia 23681-2199

June 1998

Available from the following:

NASA Center for AeroSpace Information (CASI)
7121 Standard Drive
Hanover, MD 21076-1320
(301) 621-0390

National Technical Information Service (NTIS)
5285 Port Royal Road
Springfield, VA 22161-2171
(703) 487-4650

Abstract

This report describes the formulation of a model of the dynamic behavior of the Benchmark Active Controls Technology (BACT) wind tunnel model for active control design and analysis applications. The model is formed by combining the equations of motion for the BACT wind tunnel model with actuator models and a model of wind tunnel turbulence. The primary focus of this report is the development of the equations of motion from first principles by using Lagrange's equations and the principle of virtual work. A numerical form of the model is generated by making use of parameters obtained from both experiment and analysis. Comparisons between experimental and analytical data obtained from the numerical model show excellent agreement and suggest that simple coefficient-based aerodynamics are sufficient to accurately characterize the aeroelastic response of the BACT wind tunnel model. The equations of motion developed herein have been used to aid in the design and analysis of a number of flutter suppression controllers that have been successfully implemented.

Introduction

Active control of aeroelastic phenomena, especially in the transonic speed regime, is a key technology for future aircraft design.[1] The Benchmark Active Controls Technology (BACT) project is part of NASA Langley Research Center's Benchmark Models Program[1,2] for studying transonic aeroelastic phenomena. The BACT wind tunnel model was developed to collect high quality unsteady aerodynamic data (pressures and loads) at transonic flutter conditions and demonstrate flutter suppression by using spoilers (alone and in concert with a traditional trailing edge control surface). The availability of truly multivariable control laws also provided an opportunity to evaluate the effectiveness of a controller performance evaluation (CPE) tool[3] to assess open- and closed-loop stability and controller robustness when applied to multivariable systems. An underlying requirement of these objectives was the availability of a mathematical model of the BACT dynamics.

A mathematical model is the basis for nearly all control design methods, therefore an appropriate model is essential. The importance of having a good model of the dynamic behavior which satisfies the needs of control law design and to accurately assess system performance and robustness cannot be overstated. In addition, a model is required to perform the extensive analysis and simulation that are usually required before controller implementation to assure that safety is not compromised. This is especially true in the area of aeroservoelastic testing in which failure can result in destruction of the wind tunnel model and damage to the wind tunnel.

One of the most important properties to accurately model is the frequency response in the vicinity of the key dynamics over the anticipated range of operating conditions. In the case of flutter suppression, the key dynamics occur near the flutter frequency and the operating conditions correspond to a wide range of dynamic pressures and Mach numbers representing both stable and unstable conditions. The key parametric variations associated with the uncertainties due to the assumptions and limitations of the analysis tools and other data used to build the model are also important. The development of the mathematical model of the dynamic behavior of the BACT presented herein was motivated by these factors.

Starting from first principles and by using appropriate idealizations of the structural and aerodynamic characteristics, a model was developed that includes spoiler controls and explicitly contains the key physical parameters. This report emphasizes the development of the equations of motion of the BACT wind tunnel model. A more comprehensive mathematical model that includes actuator and turbulence models is presented as well. The resulting numerical model is also validated by using several types of static and dynamic analysis.

Nomenclature

Symbols

B_0, B_1, B_2	control effectiveness matrices associated with control deflection, rate, and acceleration, respectively
b	wing semispan (distance from root to tip)
C_L, C_M	aerodynamic lift and pitching moment coefficients, respectively
$C_{L(\cdot)}$, $C_{M(\cdot)}$	derivative of lift and moment coefficients with respect to. $(\cdot)$, respectively
c	wing chord
$\bar{c}$	mean aerodynamic chord
D_s, D_a	structural and aerodynamic damping matrices, respectively
$d_{(\cdot)}$	chordwise distance from the shear center to the $(\cdot)$ sensor location
E	wind tunnel turbulence disturbance matrix
e_1	distance from origin of body fixed reference to center of gravity of BACT/PAPA body (excluding control surfaces)
e_2	distance from origin of body fixed reference to center of gravity of trailing edge control surface
e_h	distance from origin of body fixed reference to hinge line of trailing edge control surface
e_δ	distance from hinge line of trailing edge control surface to center of gravity of trailing edge control surface
g	gravitational acceleration
H_δ	aerodynamic control surface hinge moment
h	plunge or vertical deflection of wing (positive down)
I_1	angular moment of interia of BACT/PAPA body (excluding control surfaces) about the origin of the body fixed reference
I_2	angular moment of inertia of trailing edge control surface about its hinge line
K_h, K_θ, K_δ	plunge, pitch, and control surface support stiffness, respectively
K_s, K_a	structural and aerodynamic stiffness matrices, respectively
L	aerodynamic lift force
L_t	turbulence model parameter
$\ell(x)$	chordwise distance form the origin of the body fixed coordinate system to the point at which angle of attack is referenced
M	aerodynamic pitching moment, Mach number

M_s, M_a, M_g	structural and aerodynamic mass matrices, respectively
m_1	mass of BACT/PAPA body (excluding control surfaces)
m_2	mass of trailing edge control surface
$p(x,y,t)$	differential pressure (upper surface - lower surface) at the point *(x,y)* on the wing surface at time *t*
$Q_{(\cdot)}{}^{e}$	generalized externally applied force associated with generalized coordinate $(\cdot)$
$Q_{(\cdot)}{}^{nc}$	generalized nonconservative (i.e., structural damping) forces
Q_0	generalized aerodynamic force matrix at zero angle of attack
Q_T	generalized aerodynamic force matrix associated with turntable angle
q	pitch rate
$\bar{q}$	dynamic pressure
$\bar{q}_f$	flutter dynamic pressure
S	planform area of wing
s_{ij}	inertial coupling between generalized coordinates *i* and *j*
T	kinetic energy
t	time
U_g	gravitational potential energy
U_e	elastic strain energy
U_0	freestream airspeed
δW	work done by virtual displacements of generalized coordinates
w_g	normal perturbation velocity of local flow field disturbances (positive down relative to the freestream flow)
w	vector of disturbances
x	chordwise distance (positive aft from root mid-chord)
x_p	chordwise position of origin of body fixed coordinate system
x_f	chordwise position of hinge of control surface
y	spanwise distance (positive outboard from wing root)
z	displacement normal to wing chord (positive up)
α	angle of attack, turbulence model parameter
β_p	turbulence model parameter
γ_p	turbulence model parameter

δ	control surface deflection, vector of control surface deflections
δ_c	commanded control surface deflection
δ_{TE}, δ_{US}	trailing edge and upper spoiler control surface deflections, respectively
η_g	random input to turbulence model
ζ_h, ζ_θ	modal structural damping ratio, plunge and pitch, respectively
θ	pitch angle
θ_T	turntable angle
$\xi_{(\cdot)}$, ξ	generalized coordinate, vector of generalized coordinates
ω_h, ω_θ	in vacuo modal frequencies, plunge and pitch, respectively
ω_f	flutter frequency

Subscripts / Superscripts

$(\cdot)_0$	equilibrium, trim, or bias value of $(\cdot)$
$\tilde{(\cdot)}$	perturbation of $(\cdot)$
$(\cdot)_f$	flutter
$(\cdot)_{LEI}$	leading edge inboard
$(\cdot)_{LEO}$	leading edge outboard
$(\cdot)_{TE}$	trailing edge control
$(\cdot)_{TEI}$	trailing edge inboard
$(\cdot)_{TEO}$	trailing edge outboard
$(\cdot)_{US}$	upper spoiler control
$(\cdot)^e$	external
$(\cdot)^{nc}$	nonconservative

Operators

$\dot{(\cdot)}$	derivative with respect to time
$\ddot{(\cdot)}$	second derivative with respect to time
$\frac{\partial}{\partial(\cdot)}$	partial derivative with respect to. $(\cdot)$

Abbreviations

BACT	Benchmark Active Control Technology

CFD	Computational Fluid Dynamics
CPE	Controller Performance Evaluation
FFT	Fast Fourier Transform
NACA	National Advisory Council for Aeronautics
PAPA	Pitch and Plunge Apparatus
psf	pounds per square foot
rms	root mean square
TDT	Transonic Dynamics Tunnel
2-DOF	two degree of freedom

The BACT Wind Tunnel Model

The BACT wind tunnel model is a rigid rectangular wing with an NACA 0012 airfoil section.[4] A photograph of the model with physical dimensions is shown in figure 1. The wing is equipped with a trailing edge control surface and upper and lower surface spoilers that can be controlled independently via hydraulic actuators. The lower surface spoiler (not shown) is identical in size and relative location to the upper surface spoiler. The wind tunnel model is instrumented with pressure transducers, accelerometers, control surface position sensors, and hydraulic pressure transducers. The accelerometers are the primary sensors for feedback control and are located at each corner of the wing.

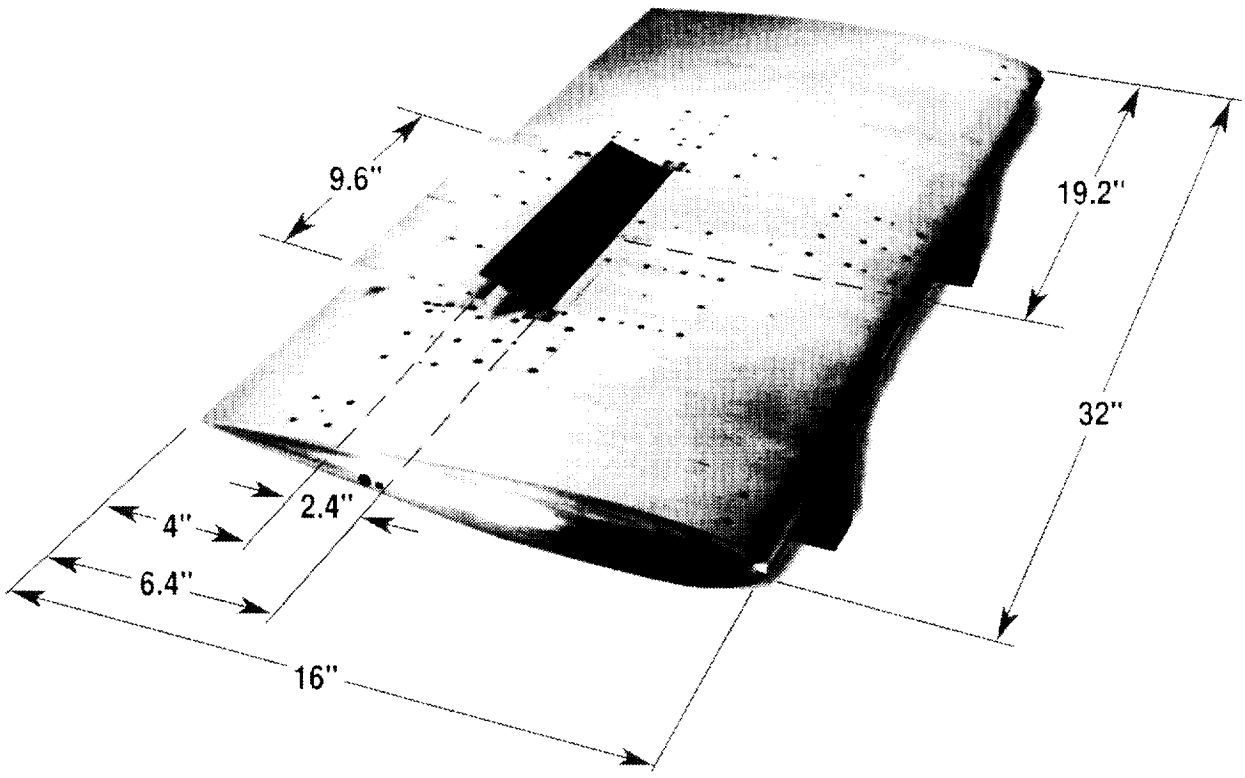

Figure 1 - BACT wing section with dimensions.

The wing is mounted to a device called the Pitch and Plunge Apparatus[4] (PAPA) which is designed to permit motion in principally two modes — rotation (or pitch), and vertical translation (or plunge). A photograph of the BACT wing mounted to the PAPA is shown in figure 2. The mass, inertia, and center of gravity location of the system can be controlled by locating masses at various points along the mounting bracket. The stiffness properties can be controlled by changing the properties of the support rods. The PAPA is instrumented with strain gauges to measure normal force and pitching moment and is mounted to a turntable that can be rotated to control the angle of attack of the wing.

The combination of the BACT wing section and PAPA mount will be referred to as the BACT system. The BACT system was precisely tuned to flutter within the operating range of the NASA Langley Transonic Dynamics Tunnel (TDT)[5] in which the system was tested. The range of Mach numbers and dynamic pressures over which flutter occurs permits the study of transonic aeroelastic phenomena. More detailed descriptions of both the BACT wing section and the PAPA mounting system can be found in references 4, 6, and 7.

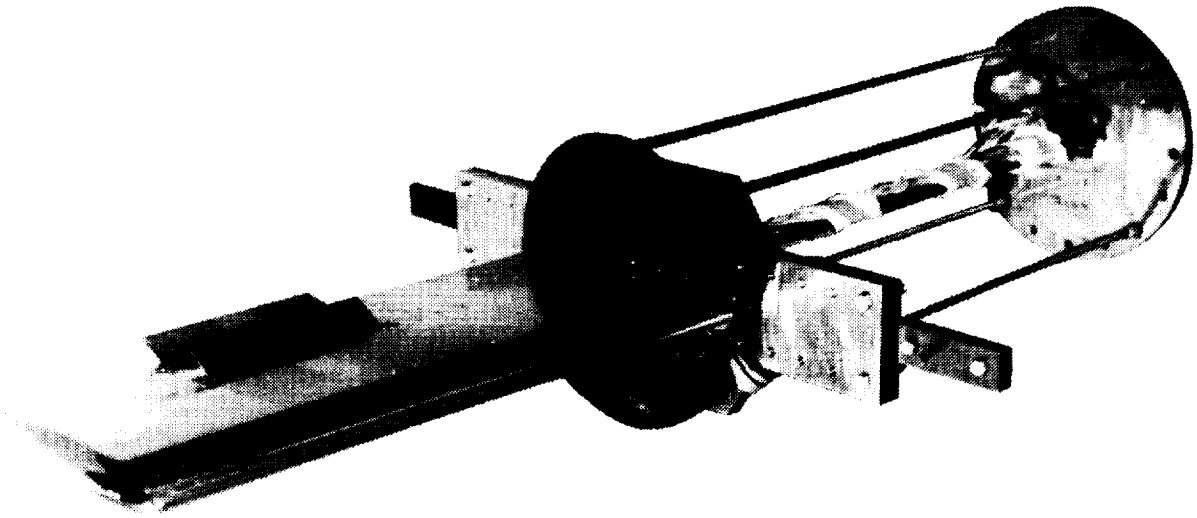

Figure 2 - Photograph of BACT wing section and PAPA mount.

Aeroelastic Equations of Motion

The BACT system has dynamic behavior very similar to the classical two degree of freedom (2-DOF) problem in aeroelasticity.[8] This similarity was exploited in the development of the aeroelastic equations of motion for the BACT system by representing it as a 2-DOF system and by using a strip theory aerodynamic approximation.[9,10] The difference between the classical 2-DOF system and the BACT system is primarily the complexity of aerodynamic behavior and presence of additional structural modes. The finite span and low aspect ratio of the BACT wing introduce significant three dimensional flow effects. The finite span of the control surfaces and their close proximity also introduce significant aerodynamic effects. Higher frequency structural degrees of freedom are associated with the PAPA mount and the fact that the wing section is not truly rigid. These effects are accounted for by various means and will be discussed subsequently.

Lagrange's equations were used to derive the equations of motion for the BACT system and the principle of virtual work was used to obtain expressions for viscous damping and the generalized aerodynamic forces. Lagrange's equations and the principle of virtual work provide a simple and straight forward method for deriving the equations of motion for aeroelastic systems.[9] Lagrange's equations readily allow one to represent motions relative to a moving frame. The principle of virtual work has the advantage

of automatically accounting for the forces of constraint and thereby greatly simplifying the determination of generalized forces.

The basic requirement for applying Lagrange's equations is that the velocity of each point in the body be represented in an inertial reference frame. The efficient application of Lagrange's equations can be facilitated by representing the inertial quantities in convenient coordinate systems and selecting an appropriate set of generalized coordinates. Once the generalized coordinates are chosen, expressions for the kinetic and potential energies are determined and Lagrange's equations are applied. The principal of virtual work is used to compute the generalized forces acting on the body. The complete set of equations of motion are then assembled. Finally, the equations of motion are used to determine the equilibrium solution and perturbation equations for the system and a numerical model appropriate for control system design is obtained.

Coordinate Axes and Generalized Coordinates

The BACT system can be idealized as a collection of four rigid bodies corresponding to each of the three control surfaces and the remaining wing/PAPA element. Figure 3 depicts the relevant quantities for the wing and the trailing edge control surface. The spoiler control surfaces were treated in an analogous fashion but are omitted here for ease of discussion.

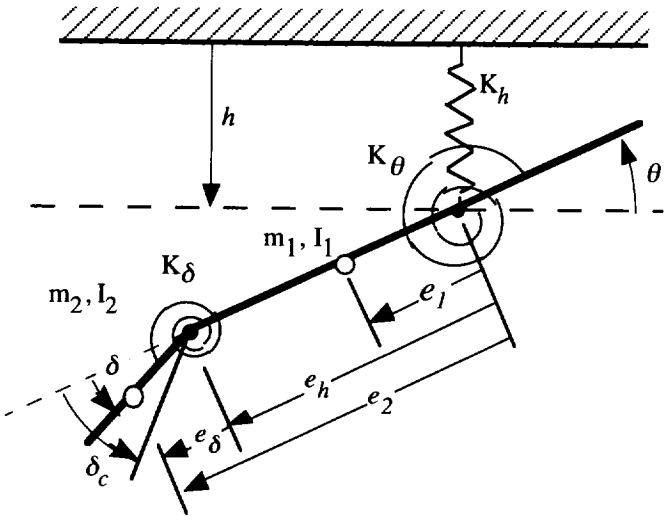

Figure 3 - Structural representation showing trailing edge control only.

There were five coordinate systems used. One coordinate system was fixed to the wing and moves with it. Another coordinate system is fixed in inertial space and oriented relative to the turntable to which the BACT system was mounted. The inertial coordinate system was chosen to coincide with the undeformed position of the body-fixed system. The three other coordinate systems are fixed to each of the control surfaces and rotate relative to the body-fixed system about the hinge of each surface.

The origin of the inertial coordinate axes is located at the shear center of the undeformed position. The origin of the body fixed coordinate axes coincides with the instantaneous shear center of the system. The origin of the control surface-fixed coordinate axes coincides with the hinge lines.

The generalized coordinates were selected to simplify the derivation of the equations of motion and were based on some key assumptions about the nature of the motion of the BACT system. The wing section and each control surface are assumed to be rigid in both the spanwise and chordwise directions. It is also assumed that the wing motion is limited to two degrees of freedom — pitch and plunge. This assumption implies that the other structural modes of the BACT system are insignificant. Investigation of the structural

vibration characteristics of the PAPA mount with a very similar wing model was shown to support this assumption.[11] The next lowest frequency for any transverse mode was more than six times the frequency of the pitch and plunge modes and outside the frequency range of interest.

Based on these assumptions the BACT requires five generalized coordinates, ξ_i $i=1,2,...,5$. The two associated with the pitch and plunge degrees of freedom were chosen to be pitch angle θ and plunge displacement h of the body fixed coordinate axes relative to the inertial coordinate axes. The three associated with the angular rotation of the control surfaces were chosen to be the trailing edge, upper spoiler, and lower spoiler control surface angles δ_{TE}, δ_{US}, and δ_{LS}, respectively. The three coordinates h, θ, and $\delta \equiv \delta_{TE}$ are depicted in figure 3 for the system in which only the trailing edge control surface is included.

Kinetic and Potential Energy

The selection of the generalized coordinates allows expressions for the kinetic and potential energies to be formulated. The kinetic energy of a body is the work required to increase its velocity from rest to some value relative to an inertial frame. By using the quantities defined in figure 3 the kinetic energy expression for the BACT system neglecting the spoiler controls can be written

$$T = \frac{1}{2}m_1(\dot{h}+e_1\dot{\theta})^2 + \frac{1}{2}I_1\dot{\theta}^2 + \frac{1}{2}m_2(\dot{h}+e_2\dot{\theta}+e_\delta\dot{\delta})^2 + \frac{1}{2}I_2(\dot{\theta}+\dot{\delta})^2. \tag{1}$$

The potential energy of a rigid body supported by pitch and plunge springs consists of two terms, the strain energy in the springs and the gravitational potential energy. The gravitational potential is defined relative to a arbitrary datum. By using the quantities defined in figure 3 and assuming the datum to be the origin of the inertial frame the gravitational potential for the BACT system is

$$U_g = -m_1 g(h+e_1\sin\theta)\cos\theta_T - m_2 g(h+e_2\sin\theta+e_\delta\sin\delta)\cos\theta_T, \tag{2}$$

where g is the gravitational acceleration and θ_T is the turntable angle.

The strain energy is the work done in going from the undeformed reference position to the deformed position. By using the quantities defined in figure 3 the strain energy for the BACT system can be written

$$U_e = \frac{1}{2}K_h h^2 + \frac{1}{2}K_\theta\theta^2 + \frac{1}{2}K_\delta(\delta-\delta_c)^2, \tag{3}$$

where K_h and K_θ are the spring constants associated with the stiffness properties of the PAPA mount and K_δ is the spring constant representing the flexibility in the structure supporting the actuator. Note that the strain energy associated with the control surface is chosen to be based on the difference between the actual and the commanded control surface rotations δ and δ_c, respectively.

The total potential energy for the BACT system is simply the sum of the gravitational potential and the strain energies in Eqns (2) and (3), respectively.

Applying Lagrange's Equations

Lagrange's equations can be expressed as

$$\frac{d}{dt}\left(\frac{\partial T}{\partial \dot{\xi}_i}\right) - \frac{\partial T}{\partial \xi_i} + \frac{\partial U}{\partial \xi_i} = Q_{\xi_i}, \tag{4}$$

where T and U are the total kinetic and potential energies of the system, ξ_i is the ith generalized coordinate, and Q_{ξ_i} is the generalized force associated with ξ_i and includes externally applied forces, nonconservative forces, and forces of constraint.

Applying the expressions for the kinetic and potential energies to Eqn (4) results in the system of equations

$$\begin{bmatrix} m & s_{h\theta} & s_{h\delta} \\ s_{h\theta} & I_\theta & s_{\theta\delta} \\ s_{h\delta} & s_{\theta\delta} & I_\delta \end{bmatrix} \begin{Bmatrix} \ddot{h} \\ \ddot{\theta} \\ \ddot{\delta} \end{Bmatrix} + \begin{bmatrix} K_h & 0 & 0 \\ 0 & K_\theta & 0 \\ 0 & 0 & K_\delta \end{bmatrix} \begin{Bmatrix} h \\ \theta \\ \delta \end{Bmatrix} = \begin{Bmatrix} 0 \\ 0 \\ K_\delta \end{Bmatrix} \delta_c + \begin{Bmatrix} m \\ s_{h\theta} \cos\theta \\ s_{h\delta} \cos\delta \end{Bmatrix} g \cos\theta_T + \begin{Bmatrix} Q_h \\ Q_\theta \\ Q_\delta \end{Bmatrix}. \tag{5}$$

The terms m, I_θ, and I_δ are the generalized masses of the pitch, plunge, and control surface modes, respectively. The terms $s_{h\theta}$, $s_{h\delta}$, and $s_{\theta\delta}$ are the inertial coupling between the generalized coordinates. These terms are related to the quantities defined in figure 3 by

$$\begin{aligned} m &\equiv m_1 + m_2, \\ I_\theta &\equiv I_1 + I_2 + m_1 e_1^2 + m_2 e_2^2, \\ I_\delta &\equiv I_2 + m_2 e_2^2, \\ s_{h\theta} &\equiv m_1 e_1 + m_2 e_2, \\ s_{h\delta} &\equiv m_2 e_\delta, \\ s_{\theta\delta} &\equiv I_2 + m_2 e_2 e_\delta. \end{aligned} \tag{6}$$

If one assumes that the control surface stiffness is very large (i.e., the deformation due to hinge load is insignificant) then Eqn (5) can be simplified by eliminating the generalized force associated with the control surface Q_δ. Assume that the control surface stiffness is very large so that

$$K_\delta \sim \frac{1}{\varepsilon}, \quad \varepsilon << 1.$$

After eliminating terms of order ε, Eqn (5) can be approximated by

$$\delta = \delta_c, \tag{7}$$

$$\begin{bmatrix} m & s_{h\theta} \\ s_{h\theta} & I_\theta \end{bmatrix} \begin{Bmatrix} \ddot{h} \\ \ddot{\theta} \end{Bmatrix} + \begin{bmatrix} K_h & 0 \\ 0 & K_\theta \end{bmatrix} \begin{Bmatrix} h \\ \theta \end{Bmatrix} = -\begin{Bmatrix} s_{h\delta} \\ s_{\theta\delta} \end{Bmatrix} \ddot{\delta} + \begin{Bmatrix} m \\ s_{h\theta} \end{Bmatrix} g \cos\theta_T + \begin{Bmatrix} Q_h \\ Q_\theta \end{Bmatrix}. \tag{8}$$

Note that the value of θ has been assumed to be small so that $\cos\theta$ is approximately unity. Also note that the inertial coupling between the wing structure and the control surface is retained in the equations.

All that remains to complete the equations of motion is to determine expressions for the generalized forces Q_h and Q_θ.

Applying the Principle of Virtual Work

The principle of virtual work can be applied to obtain expressions for the generalized forces. The basic advantage of using this method is that the forces of constraint are eliminated automatically. In addition, the principle of virtual work can be used to determine expressions for dissipative forces such as damping.

The generalized force Q_{ξ_i} can be determined from

$$Q_{\xi_i} = \frac{\partial \delta W}{\partial \delta \xi_i}, \tag{9}$$

where δW is the work done on the system by arbitrary infinitesimal (or *virtual*) displacements of the generalized coordinates $\delta\xi$. This *virtual* work includes the work done by nonconservative forces (e.g., damping) and external forces. The work done by forces of constraint are zero under virtual displacements.

Nonconservative (Damping) Forces

Structural damping is often characterized as a viscous force. Experimental data suggests that this is a reasonable assumption for the BACT system undergoing small motions.[4,6] Viscous forces are those where the force varies in proportion to the velocity at the point the force is applied but in the opposite direction. The generalized damping forces for the BACT can be represented as

$$\begin{Bmatrix} Q_h{}^{nc} \\ Q_\theta{}^{nc} \end{Bmatrix} = -\begin{bmatrix} m & s_{h\theta} \\ s_{h\theta} & I_\theta \end{bmatrix}\begin{bmatrix} 2\zeta_h\omega_h & 0 \\ 0 & 2\zeta_\theta\omega_\theta \end{bmatrix}\begin{Bmatrix} \dot{h} \\ \dot{\theta} \end{Bmatrix}. \tag{10}$$

The terms in Eqn (10) were chosen so that the damping coefficients associated with the plunge and pitch modes, ζ_h and ζ_θ, respectively, correspond to those obtained from experiment. The matrix premultiplying the diagonal damping matrix is the mass matrix from Eqn (8). The other constants ω_h and ω_θ correspond to the in vacuo vibration frequencies for the pitch and plunge modes. This so-called equivalent modal damping formulation results in a diagonal damping matrix when the system is written in modal form.

External (Aerodynamic) Forces

The externally applied forces are due to aerodynamics and result from the distributed pressures applied to the surface of the BACT wing. The virtual work for the wing can be written

$$\delta W = \int_0^b \int_{-\frac{c}{2}}^{+\frac{c}{2}} p(x,y,t)\,\delta z(x,y,t)\,dx\,dy, \tag{11}$$

where b is the wing semi-span, c is the section chord, $p(x,y,t)$ is the differential pressure distribution over the surface of the wing, and $\delta z(x,y,t)$ is a virtual displacement normal to the wing surface. Figure 4 depicts the pressure distribution for a chordwise section.

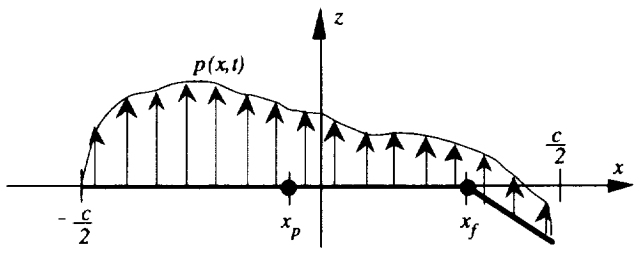

Figure 4 - Pressure distribution over wing section.

The virtual displacement δz can be written in terms of virtual displacements of the generalized coordinates h, θ, and δ as

$$-\delta z(x,y,t) = \delta h(t) + (x - x_p)\delta\theta(t) + \begin{cases} 0, & x < x_f \\ (x - x_f)\delta\delta, & x > x_f \end{cases}. \tag{12}$$

Substituting this expression in Eqn (11) and performing the differentiation described in Eqn (9) results in expressions for the generalized aerodynamic forces

$$\begin{aligned} Q_h{}^e &= \frac{\partial \delta W}{\partial \delta h} = -\int_0^b \int_{-c/2}^{+c/2} p(x,y,t)\,dx\,dy \equiv -L, \\ Q_\theta{}^e &= \frac{\partial \delta W}{\partial \delta \theta} = -\int_0^b \int_{-c/2}^{+c/2} p(x,y,t)(x - x_p)\,dx\,dy \equiv M_p, \\ Q_\delta{}^e &= \frac{\partial \delta W}{\partial \delta \delta} = -\int_0^b \int_{x_f}^{+c/2} p(x,y,t)(x - x_f)\,dx\,dy \equiv H_\delta, \end{aligned} \tag{13}$$

where L, M_p, and H_δ are the lift, pitching moment about the reference point x_p and the control surface moment about its hinge line x_f, respectively. The reference point x_p was chosen to correspond to the shear center (i.e., the origin of the body fixed coordinate system).

There are several ways in which the integrated surface pressures can be approximated in practice. If computational aerodynamic analysis results are available the integration can be approximated by using the pressures on the computational grid. If experimental force and moment data are available it can be used directly in Eqn (13) after accounting for differences in the moment reference point.

A common method of approximating the aerodynamic forces is to use stability and control derivatives. The aerodynamic forces are represented as a linear function of angle of attack, control surface deflection, and their rates by

$$\begin{aligned} L &= \bar{q}SC_L \\ &= \bar{q}S\left[C_{L_0} + C_{L_\alpha}\alpha + C_{L_\delta}\delta + \frac{\bar{c}}{2U_0}\left(C_{L_{\dot\alpha}}\dot\alpha + C_{L_q}\dot\theta + C_{L_{\dot\delta}}\dot\delta\right)\right], \end{aligned} \tag{14}$$

$$\begin{aligned} M_p &= \bar{q}S\bar{c}C_M \\ &= \bar{q}S\bar{c}\left[C_{M_0} + C_{M_\alpha}\alpha + C_{M_\delta}\delta + \frac{\bar{c}}{2U_0}\left(C_{M_{\dot\alpha}}\dot\alpha + C_{M_q}\dot\theta + C_{M_{\dot\delta}}\dot\delta\right)\right]. \end{aligned} \tag{15}$$

A description of each coefficient is presented in table 2 in the Numerical Model Parameters section. A comparable expression for the hinge moment has been omitted since the need for the generalized force associated with hinge moment in the equations of motion was eliminated in Eqn (8).

The coefficient based approach is a rather simplistic way to represent the aerodynamic forces and moments, but it is quite acceptable for the BACT system as will be seen. The need to include more sophisticated aerodynamic modeling approaches such as rational function approximations or time accurate CFD is mitigated by the fact that the reduced frequency for the BACT system is relatively low (e.g., approximately 0.04 at a flutter dynamic pressure of 150 psf using semichord as the reference length). Therefore, the lag between changes in angle of attack and the resulting lift force is not significant.

A relation between the generalized coordinates and the angle of attack is required to represent the generalized aerodynamic forces in a form consistent with the equations of motion. Here it is assumed that the wind tunnel model is rigid and that the angle of attack is the same for each spanwise position. Based on the choice of the generalized coordinates, the angle-of-attack at any chordwise point x at any time t can be represented by

$$\alpha(x,t) = \theta_T + \theta(t) + \frac{\dot{h}(t)}{U_0} + \frac{\ell(x)\dot{\theta}(t)}{U_0} - \frac{w_g(x,t)}{U_0}, \tag{16}$$

where θ_T is the turntable angle, $\ell(x)$ is the chordwise distance from the origin of body fixed coordinate system to the point at which the angle of attack is referenced (positive aft), w_g is the normal perturbation velocity of disturbances in the local flow field (positive down relative to the free stream flow), and U_0 is the freestream velocity.

By using the expression for angle of attack from Eqn (16) in Eqns (14) and (15) the generalized applied external forces can be written

$$\begin{aligned}
\begin{Bmatrix} Q_h{}^e \\ Q_\theta{}^e \end{Bmatrix} &= \bar{q}S\begin{bmatrix} -C_{L_0} \\ \bar{c}C_{M_0} \end{bmatrix} + \bar{q}S\begin{bmatrix} -C_{L_\alpha} \\ \bar{c}C_{M_\alpha} \end{bmatrix}\theta_T + \frac{\bar{q}S\bar{c}}{2U_0{}^2}\begin{bmatrix} -C_{L_{\dot{\alpha}}} & -\ell(x)C_{L_{\dot{\alpha}}} \\ \bar{c}C_{M_{\dot{\alpha}}} & \bar{c}\ell(x)C_{M_{\dot{\alpha}}} \end{bmatrix}\begin{Bmatrix} \ddot{h} \\ \ddot{\theta} \end{Bmatrix} \\
&+ \frac{\bar{q}S}{U_0}\begin{bmatrix} -C_{L_\alpha} & -\ell(x)C_{L_\alpha} - \frac{\bar{c}}{2U_0}\left(C_{L_{\dot{\alpha}}} + C_{L_q}\right) \\ \bar{c}C_{M_\alpha} & \bar{c}\ell(x)C_{M_\alpha} + \frac{\bar{c}}{2U_0}\left(C_{M_{\dot{\alpha}}} + C_{M_q}\right) \end{bmatrix}\begin{Bmatrix} \dot{h} \\ \dot{\theta} \end{Bmatrix} + \bar{q}S\begin{bmatrix} 0 & -C_{L_\alpha} \\ 0 & C_{M_\alpha} \end{bmatrix}\begin{Bmatrix} h \\ \theta \end{Bmatrix} \\
&+ \frac{\bar{q}S\bar{c}}{2U_0}\begin{bmatrix} -C_{L_{\dot{\delta}}} \\ \bar{c}C_{M_{\dot{\delta}}} \end{bmatrix}\dot{\delta} + \bar{q}S\begin{bmatrix} -C_{L_\delta} \\ \bar{c}C_{M_\delta} \end{bmatrix}\delta - \frac{\bar{q}S}{U_0}\begin{bmatrix} -\frac{\bar{c}}{2U_0}C_{L_{\dot{\alpha}}} & -C_{L_\alpha} \\ \frac{\bar{c}}{2U_0}C_{M_{\dot{\alpha}}} & \bar{c}C_{M_\alpha} \end{bmatrix}\begin{Bmatrix} \dot{w}_g \\ w_g \end{Bmatrix}.
\end{aligned} \tag{17}$$

Complete BACT Equations of Motion

Combining the generalized forces, Eqns (10) and (17), with Eqn (8) results in a complete set of equations of motion for the BACT system. The general form of the equations can be expressed as

$$\begin{aligned}
&\left(M_s - \frac{\bar{q}S\bar{c}}{2U_0{}^2}M_a\right)\ddot{\xi} + \left(D_s - \frac{\bar{q}S}{U_0}D_a\right)\dot{\xi} + \left(K_s - \bar{q}SK_a\right)\xi \\
&\quad = \bar{q}SQ_0{}^e + \bar{q}SQ_T\theta_T + M_g g\cos\theta_T + B_2\ddot{\delta} + \frac{\bar{q}S\bar{c}}{2U_0}B_1\dot{\delta} + \bar{q}SB_0\delta + \frac{\bar{q}S}{U_0}Ew,
\end{aligned} \tag{18}$$

where ξ is the vector of generalized coordinates (see Appendix), θ_T is the turntable angle, δ is the vector of control surface deflections, w is the vector of disturbance inputs (downwash velocity and acceleration - see Appendix), and $\bar{q}$ is the dynamic pressure. The definitions of the matrices M_s, M_a, M_g, D_s, D_a, K_a, K_a, Q_0, Q_T, B_0, B_1, B_2, and E are presented in the Appendix.

Notice that the effect of the aerodynamic forces is to modify the mass, damping, and stiffness properties of the system. It is this aerodynamic coupling that is the essential feature of aeroelastic systems and leads to the flutter instability. Also note that the aerodynamic matrices are explicit functions of the dynamic pressure and freestream velocity. So, for a given Mach number, the equations of motion represent a continuum of system dynamics associated with a range of dynamic pressures. This parameterization is

particularly useful for studying the stability characteristics of the system. Finally, note that there are three terms in the equations that are constant, assuming the turntable angle is fixed. These terms determine the static equilibrium of the system.

Equilibrium Solution and Perturbation Equations

The static equilibrium of the BACT system is obtained by setting all time derivatives in Eqn (18) to zero and by solving for the generalized coordinates. Doing so results in

$$\xi_0 = \left(K_s - K_a\right)^{-1}\left[Q_0{}^e + Q_T\theta_T + M_g g\cos\theta_T + B_0\delta_0\right]. \tag{19}$$

The subscript $(\cdot)_0$ on the generalized coordinate vector is used to indicate static equilibrium. The subscript $(\cdot)_0$ on the control input is used to denote a fixed reference value (e.g., bias, trim value).

The generalized coordinates can be expressed as the sum of the static (or equilibrium) part ξ_0 and a perturbation part $\tilde{\xi}$ by

$$\xi = \xi_0 + \tilde{\xi}. \tag{20}$$

The control input can be expressed as the sum of the bias or static part δ_0 and the time varying or dynamic part $\tilde{\delta}$ by

$$\delta = \delta_0 + \tilde{\delta}. \tag{21}$$

Substituting Eqns (20) and (21) into Eqn (18), by using the fact that ξ_0, θ_T, and δ_0 are constant, and by eliminating the constant terms by using Eqn (19) results in the perturbation state space equations of motion for the BACT system

$$\begin{Bmatrix} \ddot{\tilde{\xi}} \\ \dot{\tilde{\xi}} \end{Bmatrix} = \begin{bmatrix} -\left(M_s - \frac{\bar{q}S\bar{c}}{2U_0{}^2}M_a\right)^{-1}\left(K_s - \bar{q}SK_a\right) & -\left(M_s - \frac{\bar{q}S\bar{c}}{2U_0{}^2}M_a\right)^{-1}\left(D_s - \frac{\bar{q}S}{U_0}D_a\right) \\ I & 0 \end{bmatrix} \begin{Bmatrix} \dot{\tilde{\xi}} \\ \tilde{\xi} \end{Bmatrix}$$
$$+ \begin{bmatrix} -\left(M_s - \frac{\bar{q}S\bar{c}}{2U_0{}^2}M_a\right)^{-1}B_2 \\ 0 \end{bmatrix} \ddot{\tilde{\delta}} + \begin{bmatrix} -\left(M_s - \frac{\bar{q}S\bar{c}}{2U_0{}^2}M_a\right)^{-1}\frac{\bar{q}S\bar{c}}{2U_0}B_1 \\ 0 \end{bmatrix} \dot{\tilde{\delta}} \tag{22}$$
$$+ \begin{bmatrix} -\left(M_s - \frac{\bar{q}S\bar{c}}{2U_0{}^2}M_a\right)^{-1}\bar{q}SB_0 \\ 0 \end{bmatrix} \tilde{\delta} + \begin{bmatrix} -\left(M_s - \frac{\bar{q}S\bar{c}}{2U_0{}^2}M_a\right)^{-1}\frac{\bar{q}S}{U_0}E \\ 0 \end{bmatrix} w.$$

While the form of the equations that appear in Eqn (18) describe the complete motion of the system, it is the form of the equations of motion presented in Eqn (22) that are most readily applicable to typical control system design methods. Note that even though Eqn (22) was derived for a single control surface, extension to multiple control surfaces is straight forward since there is no inertial coupling between the various control surfaces of the BACT. There is, however, aerodynamic coupling between the control surfaces due to their close proximity. The form of the aerodynamic force expressions allows some effects of coupling to be approximated within the stability and control derivative terms by altering the derivative values to account for control surface biases. For example, the effectiveness of the trailing edge control surface ($C_{L_{TE}}, C_{M_{TE}}$) can be adjusted to account for the influence of biases of the other surfaces. However, perturbation effects (i.e., changes in the control effectiveness due to motion of the other surfaces about their bias values) are ignored in this approach.

Numerical Model Parameters

A numerical form of the equations of motion of the BACT system was obtained by substituting numerical values for each parameter in the equations of motion developed above. Most of the parameter values were obtained from experimental data but some of the aerodynamic data were obtained from numerical analysis using computational aerodynamics.

The mass and inertia parameters were obtained by measuring the mass, stiffness, and damping properties of the various components of the BACT system. The geometric parameters (e.g., centers of gravity, shear center, sensor locations, and aerodynamic reference quantities) were also obtained directly from measurement of the BACT and PAPA components. The mass, stiffness, and damping parameter values that were used in the numerical form of the BACT equations of motion are presented in table 1. The center of gravity and shear center were essentially coincident and located at the mid-chord point of the wing.

The static aerodynamic parameters were determined from experimental data that were obtained from a previous wind tunnel test in which the BACT wing was mounted on a force and moment balance.[7] Force and moment data for various angles of attack and control surface positions were used to compute most of the stability and control derivatives using finite differences. The upper spoiler control derivatives were obtained relative to a bias deflection (5 to 10 degrees) about which the spoiler was deflected to control the system. The spoiler bias allows both positive and negative control inputs to be produced.

Table 1 - Mass, Stiffness, and Damping Parameters

Symbol	Description	Value	Units
m	mass	6.08	slug
I_θ	pitch inertia	2.80	slug-ft^2
K_h	plunge stiffness	2686	lb/ft
K_θ	pitch stiffness	3000	lb-ft
ω_h	in vacuo plunge frequency	21.01	rad/sec
ω_θ	in vacuo pitch frequency	32.72	rad/sec
ζ_h	plunge damping ratio	0.0014	-
ζ_θ	pitch damping ratio	0.0010	-
$s_{h\theta}$	pitch-plunge inertial coupling	0.0142	slug-ft
$s_{h\delta TE}$	plunge-TE inertial coupling	0.00288	slug-ft
$s_{\theta\delta_{TE}}$	pitch-TE inertial coupling	0.00157	slug-ft^2
$s_{h\delta_{US}}$	plunge-US inertial coupling	0.00039	slug-ft
$s_{\theta\delta_{US}}$	pitch-US inertial coupling	9.8e-05	slug-ft^2

Sufficient experimental data were only available to quantify the trailing edge and upper spoiler control surface aerodynamic characteristics. Available data for the lower spoiler were not complete enough to characterize its aerodynamics. In addition, there were insufficient data to account for aerodynamic coupling between the spoiler and trailing edge control. Therefore, the numerical model is limited to the trailing edge and upper spoiler surfaces with no aerodynamic coupling between controls (i.e., the influence of spoiler bias on trailing edge control effectiveness is ignored).

The dynamic derivatives (e.g., C_{M_q} and $C_{L_{\dot{\alpha}}}$) were obtained from computational aerodynamic analysis. Analytical values were used because they were available from models previously generated using ISAC.* However, the dynamic derivatives associated with spoiler-surface deflection rate and acceleration were not available from these models and so all the control surface rate and acceleration derivatives were assumed to be zero.

The numerical values for the static and dynamic stability and control derivatives are presented in table 2. These values were determined at a single Mach number of 0.77 and a single dynamic pressure of 143 psf. The moment coefficients are referenced relative to the shear center that coincides with the mid-chord

Table 2 - Aerodynamic Parameters

Symbol	Description	Value	Source
C_{L_0}	lift at zero angle of attack	0	experiment
C_{M_0}	pitching moment at zero angle of attack	0	experiment
C_{L_α}	lift curve slope	4.584	experiment
C_{M_α}	moment curve slope	1.490	experiment
$C_{L_{\dot{\alpha}}}$	plunge damping due to angle of attack rate	-3.1054	analysis
C_{L_q}	plunge damping due to pitch rate	2.5625	analysis
$C_{M_{\dot{\alpha}}}$	pitch damping due to angle of attack rate	-2.6505	analysis
C_{M_q}	pitch damping due to pitch rate	-0.4035	analysis
$C_{L_{\delta_{TE}}}$	TE lift effectiveness	0.63	experiment
$C_{M_{\delta_{TE}}}$	TE moment effectiveness	-0.0246	experiment
$C_{L_{\delta_{US}}}$	US lift effectiveness	0.22	experiment
$C_{M_{\delta_{US}}}$	US moment effectiveness	0.0573	experiment
ℓ	distance between shear center and aerodynamic center	$-0.175\,\bar{c}$	experiment
S	planform area, (ft^2)	3.55	experiment
$\bar{c}$	mean aerodynamic chord, (ft)	1.33	experiment

* ISAC (or Integration of Structures, Aerodynamics, and Controls) is a tool for modeling aeroelastic aircraft for application to control system analysis and design.[12]

point of the wing. Finally, note that the expression for the generalized aerodynamic forces in Eqn (17) requires the selection of an angle of attack reference point $\ell(x)$ (i.e., the distance between the shear center and the point at which the angle of attack of the wing is measured). The aerodynamic center location based on the experimental lift and moment curve slopes was used as the angle of attack reference. This point varied with Mach number but was near the 30% chord location at Mach 0.77 and for most other operating conditions as well.

The numerical form of the matrices that appear in Eqn (18) that use the values presented in tables 1 and 2 are presented in the Appendix. Note that since the model is parameterized by $\bar{q}$ and U_0, a continuum of numerical state space models of the form in Eqn (22) can be generated. However, these models are all associated with the single Mach number at which the aerodynamic data were obtained.

Actuator and Turbulence Models and the Output Equation

The equations of motion alone are not sufficient to describe the dynamic behavior of the BACT system. While the 2-DOF system structure is sufficient to describe the basic aeroelastic properties of the BACT system, additional elements are necessary to develop a model suitable for control system design. The relative magnitude of the dynamic response is determined by the nature of the disturbance environment and influences the control activity required to achieve the desired level of closed-loop performance. Therefore, a characterization of the turbulence environment in the TDT is needed, i.e., a turbulence model. The ability of the control surfaces to produce the desired activity is dependent on the dynamic response characteristics of the actuators including bandwidth, position and rate limits, and other nonlinearities. Therefore, characterizations of the actuator dynamics are also needed, i.e., actuator models. Finally, a set of measurement signals is required to provide the basis for feedback control. An output equation relating the generalized coordinates to the measurement variables is therefore required. It is the combination of the actuator models, the turbulence model, output equation, and the aeroelastic equations of motion that determine the degree to which a control system will be able to achieve a desired level of performance and robustness.

Actuator Models

Actuator models of the BACT wind tunnel model were obtained from experimental data by using a simple parameter estimation process described in reference 13. This process was used to select the parameters of a second order actuator model to minimize the frequency response error over the frequency range of interest. The actuator transfer function model is

$$\frac{\delta(s)}{\delta_c(s)} = \frac{k\omega_a{}^2}{s^2 + 2\zeta_a\omega_a s + \omega_a{}^2}, \tag{23}$$

where k is a gain, and ω_a and ζ_a are frequency and damping, respectively. The parameter values resulting from the parameter estimation process are presented in table 3. A state space form of the second order actuator model and the numerical matrices for the trailing edge control surface and the upper spoiler actuators are presented in the Appendix.

Other factors that have a significant affect on control system design are the position and rate limits of the actuators and nonlinearities such as dead zone and backlash. The position limits for the trailing edge control surface and the spoiler-surfaces were approximately 12 degrees and 45 degrees , respectively. The rate limits, dead zone, and backlash have not yet been determined.

Table 3 - BACT Actuator Model Parameters

Symbol	Description	Value	Units
k_{TE}	TE actuator gain	1.02	deg/deg
ζ_{TE}	TE damping ratio	0.56	-
ω_{TE}	TE frequency	165.3	rad/sec
k_{US}	US actuator gain	1.16	deg/deg
ζ_{US}	US damping ratio	0.85	-
ω_{US}	US frequency	164.0	rad/sec

Turbulence Model

A model of the turbulence environment within the TDT was developed in reference 13 using power spectrum data. The model structure is that of a Dryden spectrum with the parameters adjusted to approximate the desired power spectral density. The transfer function form of the turbulence model is

$$\frac{w_g(s)}{\eta_g(s)} = \frac{2\pi\sqrt{\alpha\beta}}{\gamma} \frac{\left(s + \frac{2\pi}{\sqrt{\beta}}\right)}{\left(s^2 + \frac{4\pi}{\sqrt{\gamma}}s + \frac{4\pi^2}{\gamma}\right)} \tag{24}$$

where

$$\beta = \beta_p\left(\frac{2\pi L_t}{U_0}\right)^2 , \quad \gamma = \gamma_p\left(\frac{2\pi L_t}{U_0}\right)^2 .$$

The output w_g is the downwash disturbance velocity that appears in Eqns (16) and (17). The input η_g is a normally distributed univariate random variable. Table 4 presents a range of values for the turbulence model parameters. Note that the parameter values are based on data collected in an air medium, not the medium in which the BACT was tested (i.e., R-12) and so the reference speed, U_0, corresponds to a different Mach number. No data at the appropriate operating conditions is available. The preferred reference speed value is 400 fps because it is close to the test conditions and correlates best with experimental data. The preferred value was used to perform the disturbance analysis presented in the next section. A state space form of the turbulence model and the corresponding numerical matrices are presented in the Appendix

Table 4 - TDT Turbulence Model Parameters

	Reference Speed, U_0(fps)			
Parameter	100	200	300	400*
α	0.01	0.025	0.007	0.082
β_p	0.477	0.475	0.521	0.667
γ_p	0.546	0.464	0.497	0.533
L_t	3.261	3.71	3.391	4.163

* Preferred reference speed value for analysis and simulation.

Output Equation

The BACT system has four accelerometers, one mounted in each corner of the rectangular wing. These accelerometers sense vertical acceleration measured in g's, positive up (opposite to the sign convention for plunge, h). The acceleration at any point on the BACT wing, excluding control surfaces, has the form

$$\ddot{z}(x,y) = \frac{-\left[\ddot{h} + d_i \ddot{\theta}\right]}{g}, \tag{25}$$

where h and θ are the generalized coordinates, d_i is the chordwise distance from the shear center to the location of the ith sensor, and g is the gravitational acceleration. Table 5 presents the chordwise distance (positive aft) between the shear center and the accelerometer for each of the four accelerometers — leading edge inboard (LEI), leading edge outboard (LEO), trailing edge inboard (TEI), and trailing edge outboard (TEO).

Table 5 - Accelerometer Locations

Accelerometer Location	d_{LEI}	d_{LEO}	d_{TEI}	d_{TEO}
Distance (ft)	-0.599	-0.599	0.433	0.420

All the components described above were combined to form the complete numerical model of the BACT system. The following section addresses a variety of analyses that were performed to assess the accuracy and validity of the numerical model.

Validation of Numerical Model

There are many ways to assess the validity of the BACT numerical model. In this section a few comparisons are made between the properties of the numerical model and the actual BACT wind tunnel data. These assessments can be broken down into two categories — static properties and dynamic properties. The static properties assess the characteristics of the equilibrium solutions. The dynamic properties assess the key response characteristics of the system in the context of flutter behavior and frequency response.

Static Properties

The equilibrium position (pitch and plunge) of the BACT system depends on the turntable angle and wind tunnel operating conditions and represents a balance between the elastic and aerodynamic forces acting on the wing. Good agreement between the equilibrium position of the wind tunnel model and the equilibrium solution of the numerical model would indicate that the stiffness (structural and aerodynamic) and control surface effectiveness properties are well modeled.

Parameters that were recorded during the wind tunnel tests include turntable angle, control surface biases, and pitch angle (plunge position was not measured). In addition, the test conditions (i.e., Mach number, dynamic pressure, and control surface positions) were recorded. By using these quantities in Eqn (19), one can determine the equilibrium pitch and plunge position of the BACT system for comparison with experimental data.

Table 6 presents the computed and measured pitch angle for a small representative set of test conditions. The error in equilibrium pitch angle is less than 5 percent for all but one point. In addition, the

trends are consistent; increasing the turntable angle increases the pitch angle, deflecting the upper spoiler upward decreases the pitch angle, and deflecting the trailing edge control downward decreases the pitch angle.

Table 7 presents the computed and measured pitch angle increments due to the changes in turntable angle and control surface deflections from table 6. The size of the pitch angle increments due to turntable angle and spoiler deflection are consistent. The main discrepancy is that the pitch angle increment due to trailing edge control deflection from the experimental data is five times higher than from the numerical model. The source of the discrepancy could not be identified due to a lack of data. However, the difference could be due to experimental error or inaccurate modeling of trailing edge control effectiveness and/or stiffness of the PAPA mount (the parameters involved in balancing the aerodynamic and structural pitching moments). Experimental error is a more likely cause for the differences because the trailing edge control derivatives and the structural stiffness that were used in the numerical model were determined from experimental data and should accurately characterize the static properties of the system.

Table 6 - Static Equilibrium Position Comparison

Mach Number	Dynamic Pressure (psf)	θ_T (deg)	δ_{TE} (deg)	δ_{US} (deg)	θ_{exp} (deg)	θ_{model} (deg)	$\Delta\theta$ (%)
.65	112	1.6	0	0	2.1	2.17	3.3
.65	115	1.6	0	-10	2.0	2.05	2.5
.70	126	1.6	0	0	2.4	2.28	-5.0
.70	126	1.6	10	0	2.0	2.20	10.0
.77	120	1.4	0	0	2.0	1.95	-2.5
.77	120	4.5	0	0	6.0	6.27	4.5

Table 7 - Static Equilibrium Sensitivity Comparison

Mach Number	Dynamic Pressure (psf)	$\Delta\theta_T$ (deg)	$\Delta\delta_{TE}$ (deg)	$\Delta\delta_{US}$ (deg)	$\Delta\theta_{exp}$ (deg)	$\Delta\theta_{model}$ (deg)
.65	112	0	0	10	0.1	0.12
.70	126	0	-10	0	0.4	0.08
.77	120	-3.1	0	0	-4.0	-4.32

Dynamic Properties

A major concern in using the numerical model for control system design is the ability of the model to accurately represent the transition to flutter including the frequency and dynamic pressure of the flutter onset. Another concern is the fidelity of the model from a frequency response perspective because of the relationship between the frequency response and the design of the control system. Finally, the level of response due to turbulence is an important issue because the maximum level of control activity depends directly on the level of response of the wind tunnel model to turbulence. Each of these properties were reviewed and compared with experimental data (and numerical models generated with ISAC where possible) to assess the validity of the numerical model. Note that the ISAC-based models were not corrected using the static structural and aerodynamic data that was used to obtain the numerical model discussed herein.

Flutter Properties

The BACT wind tunnel model experienced flutter in the TDT at a dynamic pressure of approximately 148 psf at a Mach number of 0.77. The flutter dynamic pressure for the numerical model is 150.8 psf. The uncorrected ISAC generated models indicate flutter occurs between 156 and 163 psf. The flutter frequency of the BACT wind tunnel model is approximately 4 hertz. At the same operating condition the flutter frequency of the numerical model is 4.16 hertz. The uncorrected ISAC generated models indicate the flutter frequency to be approximately 4.22 hertz.

In terms of the flutter dynamic pressure and frequency at the Mach number for which aerodynamic data were available, the numerical model of the BACT system developed herein (and the ISAC-based models) gives excellent results.

Transfer Function Comparisons

One of the most important measures of model fidelity for control system design is the frequency response. In order to effectively design a control system to stabilize a flutter mode the design model must accurately characterize the dynamic behavior of the aeroelastic system over a fairly wide range of dynamic pressures from stability to neutral stability to instability.

Figures 5 and 6 show representative frequency responses for the numerical model and the actual wind tunnel model. The operating conditions corresponds to a subsonic Mach number and dynamic pressure of 125 psf, well below flutter. In figure 5 the output is trailing edge accelerometer and the input is trailing edge control deflection. In figure 6 the output is trailing edge accelerometer and the input is upper spoiler control deflection. The frequency response of an uncorrected ISAC-based model is also presented in figure 5 for comparison. Note that ISAC cannot model spoilers and so no ISAC comparison can be made in figure 6. The experimental transfer function for the upper spoiler was obtained by operating the spoiler about a bias. That is, the spoiler was given a static deflection (typically between five and ten degrees) and oscillated symmetrically about the bias. The frequency responses of the other accelerometers are comparable to those shown here.

There is excellent correlation between the experimentally obtained frequency responses and those of the numerical model. The model clearly captures the key aspects of the dynamic response of the BACT system at the subcritical dynamic pressure of 125 psf. There are, however, some discrepancies in the frequency of the magnitude peak near 3.5 hertz and in the phase characteristics. However, these differences are typical of aeroelastic systems and can be attributed to modeling errors and/or artifacts of using FFT's to generate frequency responses from experimental data.

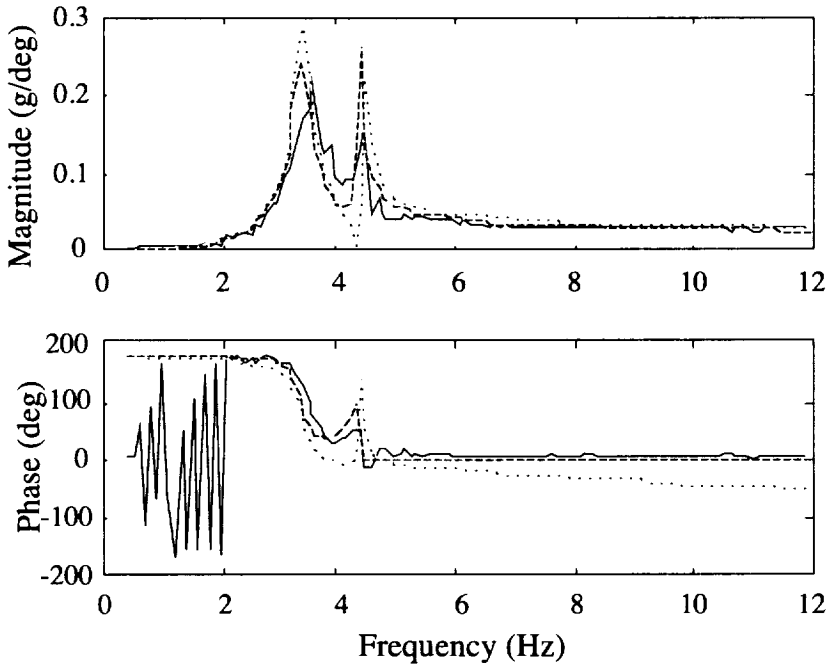

Figure 5 - Frequency response of trailing edge inboard accelerometer due to trailing edge control: $\bar{q}$ = 125 psf. (solid - experiment, dash - model, dot - ISAC).

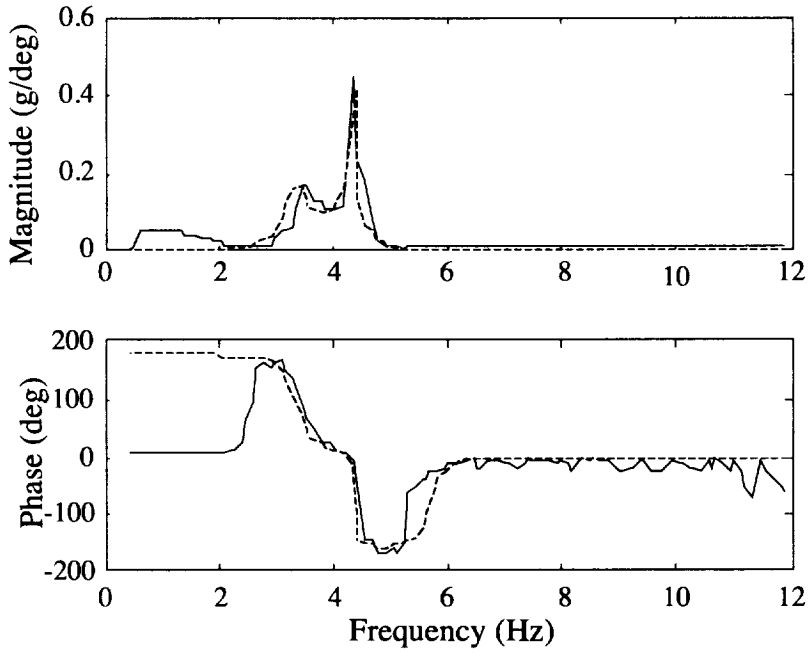

Figure 6 - Frequency response of trailing edge inboard accelerometer due to upper spoiler control: $\bar{q}$ = 125 psf (solid - experiment, dash - model).

Open-Loop RMS Accelerations

It is important for the numerical model to accurately characterize the response of the system to disturbances because disturbance response determines the control activity required to achieve the desired level of closed-loop performance. The disturbance source for the BACT system is wind tunnel turbulence. One measure of the degree to which the numerical model characterizes the effects of turbulence is rms acceleration. Table 8 presents rms trailing edge inboard acceleration at two dynamic pressures. The data are based on normalized dynamic pressure expressed as a fraction of the flutter dynamic pressure, $\bar{q}_f$. Normalization is needed because of the differences in the flutter dynamic pressure from the experiment and the numerical model. The reference speed used to scale the turbulence model is 400 fps and is consistent with the speed of the flow in the wind tunnel.

Table 8 - Comparison of RMS Trailing edge Acceleration

q_{norm} (psf)	RMS Trailing Edge Acceleration (g)		% Error
	Experiment	Model	
$0.75\,\bar{q}_f$	0.0207	0.0188	-9.2
$0.90\,\bar{q}_f$	0.0340	0.0350	2.9

Note that there is a Mach number mismatch between the experimental data and the model-based data since the aerodynamic parameter values in the numerical model are based on data collected at Mach 0.77 and the experimental data was obtained for Mach numbers of 0.63 and 0.71. The good agreement in the response level implies that the numerical model can be used to effectively assess rms response.

Comments

Based on the accuracy of the flutter properties, the subcritical frequency responses, and rms disturbance response, it is reasonable to expect the model to characterize the dynamic response of the BACT system over the anticipated range of operating conditions and is appropriate for control system design. However, the discrepancies identified above should be considered during control system design and dynamic analysis. For example, uncertainty models used in robust multivariable control system design could characterize uncertainty in the pitch effectiveness of the trailing edge control surface, the differences in magnitude and phase of the system frequency responses, and the differences in flutter dynamic pressure and frequency.

A MATLAB/SIMULINK* implementation of the wind tunnel model, actuator models, turbulence model, and digital controller effects has been developed for the purpose of evaluating and analyzing the dynamic behavior of the BACT system.[14] It has been used by several researchers to aid in the design and analysis of flutter suppression controllers. A variety of classical, H_∞, μ-synthesis, neural network, and adaptive controllers have been designed using the numerical model and have been successfully tested in the Langley Transonic Dynamics Tunnel.[15,16,17]

Concluding Remarks

The dynamic model of the Benchmark Active Control Technology (BACT) wind tunnel model presented herein has many advantages over a purely numerically derived model. It is analytical and

* MATLAB and SIMULINK are registered trademarks of The MathWorks, Inc.

parametric in nature and therefore lends itself to sensitivity and uncertainty analysis. Because the aerodynamic effects are represented in derivative form, experimental data can readily be substituted for analysis-based data. A major advantage of the modeling approach is that it allows experimental stability and control derivative data to be used to model spoiler aerodynamics. The modular form of the model also allows various components of the model to be modified or replaced. This is very useful in cases where actuator models and turbulence models are modified or updated.

The BACT model and test data are also being developed as a case study package for educational use. The relatively simple structure of the BACT system coupled with the availability of extensive and detailed experimental data make the BACT an excellent candidate for additional study of dynamics and control of aeroelastic systems.

Acknowledgment

The author wishes to acknowledge Rob Scott, Sheri Hoadley, Carol Wieseman, Robert Bennett, Robert Sleeper, and the entire BACT team without whose help this work could not have been accomplished.

References

[1] Durham, M.H.; Keller, D.F.; Bennett, R.M.; and Wieseman, C.D.: A Status Report on a Model for Benchmark Active Controls Testing. AIAA Paper No. 91-1011.

[2] Bennett. R.M.; Eckstrom, C.V.; et al.: The Benchmark Aeroelastic Models Program - Description and Highlights of Initial Results. NASA TM-104180, Dec. 1991.

[3] Wieseman, C.D.; Hoadley, S.T.; and McGraw, S.M.: On-Line Analysis Capabilities Developed to Support Active Flexible Wing Wind Tunnel Model. *Journal of Aircraft*. Vol. 23, No. 1. pp. 39-44. Jan.-Feb. 1995.

[4] Rivera, Jr., J.A.; Dansberry, B.E.; et al.: NACA 0012 Benchmark Model Experimental Flutter Results with Unsteady Pressure Distributions. AIAA Paper No. 92-2396. 33rd AIAA/ASME/ ASCE/AHS/ASC Structures, Structural Dynamics, and Materials Conference. Dallas, TX, April 1992.

[5] Baals, D.D. and Corliss, W.R.: Wind Tunnels of NASA. NASA SP-440. pp. 79-81. 1981.

[6] Rivera, Jr., J.A.; Dansberry, B.E.; Durham, M.H.; Bennett, R.M.; and Silva, W.A.: Pressure Measurements on a Rectangular Wing with a NACA 0012 Airfoil During Conventional Flutter. NASA TM-104211, July 1992.

[7] Scott, R.C.; Hoadley, S.T.; and Wieseman, C.D.: The Benchmark Active Controls Technology Model Aerodynamic Data. AIAA Paper No. 97-0829. Presented at the 35th Aerospace Sciences Meeting and Exhibit, Reno, Nevada. January 6-10, 1997.

[8] Bisplinghoff, R.L. and Ashley, H.: *Principles of Aeroelasticity*. Dover Publications, Inc., New York. 1962.

[9] Waszak, M.R. and Schmidt, D.K.: Flight Dynamics of Aeroelastic Vehicles. *Journal of Aircraft*. pp. 563-571. Vol. 25, No 6. June 1988.

[10] Yates, C.E. Jr.: Modified-Strip-Analysis Method for Predicting Wing Flutter at Subsonic to Hypersonic Speeds. *Journal of Aircraft*. Vol. 2, No. 1, pp. 25-29. Jan.-Feb. 1966.

[11] Dansberry, B.E.; Durham, M.H.; Bennett, R.M.; Turnock, D.L.; Silva, W.A.; and Rivera, Jr., J.A.: Physical Properties of the Benchmark Models Program Supercritical Wing. NASA TM-4457. September 1993.

[12] Adams, W.M.: ISAC: A Tool for Aeroservoelastic Modeling and Analysis. NASA TM-109031. December, 1993.

[13] Waszak, M.R. and Fung, J.: Parameter Estimation and Analysis of Actuators for the BACT Wind Tunnel Model. AIAA Paper No. 96-3362. AIAA Atmospheric Flight Mechanics Conference. San Diego, CA. July 29-31, 1996.

[14] Waszak, M.R.: BACT Simulation User Guide. NASA TM-97-206252. November 1997.

[15] Waszak, M.R.: Robust Multivariable Flutter Suppression for the Benchmark Active Control Technology (BACT) Wind Tunnel Model. Proceedings of the Eleventh Symposium on Structural Dynamics and Control. Blacksburg, VA. May 12-14, 1997.

[16] Haley, P.; Soloway, D.: Generalized Predictive Control for Active Flutter Suppression. IEEE Control Systems Magazine. Vol. 17 No. 4, August 1997, pp. 64-70.

[17] Mukhopadhyay, V.: Transonic Flutter Suppression Control Law Design, Analysis and Wind-Tunnel Test Results. Presented at the 2nd International Conference on Nonlinear Problems in Aviation and Aerospace. Daytona Beach, FL. April 29 - May 1, 1998.

Appendix

Definition of Symbols for Matrix Form of BACT Equations of Motion

Vector of generalized coordinates -

$$\xi \equiv \begin{Bmatrix} h \\ \theta \end{Bmatrix} \tag{A1}$$

Vector of control surface inputs -

$$\delta \equiv \begin{Bmatrix} \delta_{TE} \\ \delta_{US} \end{Bmatrix} \tag{A2}$$

Vector of disturbance inputs -

$$w \equiv \begin{Bmatrix} \dot{w}_g \\ w_g \end{Bmatrix} \tag{A3}$$

Structural, aerodynamic, and inertial coupling mass matrices -

$$M_s \equiv \begin{bmatrix} m & s_{h\theta} \\ s_{h\theta} & I_\theta \end{bmatrix} \qquad M_a \equiv \begin{bmatrix} -C_{L_{\dot{\alpha}}} & -\ell(x)C_{L_{\dot{\alpha}}} \\ \bar{c}C_{M_{\dot{\alpha}}} & \bar{c}\ell(x)C_{M_{\dot{\alpha}}} \end{bmatrix} \qquad M_g \equiv \begin{bmatrix} m \\ s_{h\theta} \end{bmatrix} \tag{A4}$$

Structural and aerodynamic damping matrices -

$$D_s \equiv -M_s \begin{bmatrix} 2\zeta_h\omega_h & 0 \\ 0 & 2\zeta_\theta\omega_\theta \end{bmatrix} \qquad D_a \equiv \begin{bmatrix} -C_{L_\alpha} & -\ell(x)C_{L_\alpha} - \dfrac{\bar{c}}{2U_0}\left(C_{L_{\dot{\alpha}}} + C_{L_q}\right) \\ \bar{c}C_{M_\alpha} & \bar{c}\ell(x)C_{M_\alpha} + \dfrac{\bar{c}}{2U_0}\left(C_{M_{\dot{\alpha}}} + C_{M_q}\right) \end{bmatrix} \tag{A5}$$

Structural and aerodynamic stiffness matrices -

$$K_s \equiv \begin{bmatrix} K_h & 0 \\ 0 & K_\theta \end{bmatrix} \qquad K_a \equiv \begin{bmatrix} 0 & -C_{L_\alpha} \\ 0 & C_{M_\alpha} \end{bmatrix} \tag{A6}$$

Generalized static aerodynamic force matrices -

$$Q_0{}^e \equiv \begin{bmatrix} -C_{L_0} \\ \bar{c}C_{M_0} \end{bmatrix} \qquad Q_T \equiv \begin{bmatrix} -C_{L_\alpha} \\ \bar{c}C_{M_\alpha} \end{bmatrix} \tag{A7}$$

Control effectiveness matrices -

$$B_0 \equiv \begin{bmatrix} -C_{L_{\delta TE}} & -C_{L_{\delta US}} \\ \bar{c}C_{M_{\delta TE}} & \bar{c}C_{M_{\delta US}} \end{bmatrix} \qquad B_1 \equiv \begin{bmatrix} -C_{L_{\dot{\delta} TE}} & -C_{L_{\dot{\delta} US}} \\ \bar{c}C_{M_{\dot{\delta} TE}} & \bar{c}C_{M_{\dot{\delta} US}} \end{bmatrix} \qquad B_2 \equiv -\begin{bmatrix} s_{h\delta TE} & s_{h\delta US} \\ s_{\theta\delta TE} & s_{\theta\delta US} \end{bmatrix} \tag{A8}$$

Numerical Form of Matrices in BACT Equations of Motion

Structural, aerodynamic, and inertial coupling mass matrices -

$$M_s \equiv \begin{bmatrix} 6.0843 & 0.0142 \\ 0.0142 & 2.8017 \end{bmatrix} \qquad M_a \equiv \begin{bmatrix} 1.5532 & -0.2712 \\ -1.3253 & 0.2319 \end{bmatrix} \qquad M_g \equiv \begin{bmatrix} 6.0843 \\ 0.0142 \end{bmatrix} \tag{A9}$$

Structural and aerodynamic damping matrices -

$$D_s \equiv \begin{bmatrix} 0.3579 & 0.0009 \\ 0.0008 & 0.1843 \end{bmatrix} \qquad D_a \equiv \begin{bmatrix} -4.5840 & 1.0739 \\ 1.490 & -1.7877 \end{bmatrix} \tag{A10}$$

Structural and aerodynamic stiffness matrices -

$$K_s \equiv \begin{bmatrix} 2686 & 0 \\ 0 & 3000 \end{bmatrix} \qquad K_a \equiv \begin{bmatrix} 0 & -4.5840 \\ 0 & 1.4900 \end{bmatrix} \tag{A11}$$

Generalized static aerodynamic force matrices -

$$Q_0{}^e \equiv \begin{bmatrix} 0 \\ 0 \end{bmatrix} \qquad Q_T \equiv \begin{bmatrix} -4.584 \\ 1.987 \end{bmatrix} \tag{A12}$$

Control effectiveness matrices -

$$B_0 \equiv \begin{bmatrix} -0.6300 & -0.2200 \\ -0.0246 & 0.0573 \end{bmatrix} \qquad B_1 \equiv \begin{bmatrix} 0 & 0 \\ 0 & 0 \end{bmatrix} \qquad B_2 \equiv -\begin{bmatrix} -0.0029 & -0.00039 \\ -0.0016 & -0.00010 \end{bmatrix} \tag{A13}$$

State Space Matrices for Actuator Models

The state space form for the actuator models is

$$\begin{aligned} \dot{x}_a &= A_a x_a + B_a \delta_c \\ \begin{bmatrix} \ddot{\delta} \\ \dot{\delta} \\ \delta \end{bmatrix} &= C_a x_a + D_a \delta_c \end{aligned} \tag{A14}$$

Note that the output of the model consists the acceleration, rate, and position of the control surface. All three are used as input to the BACT equations of motion.

The state space matrices for the trailing edge control surface actuator are

$$A_{a_{TE}} = \begin{bmatrix} -1.8514e+02 & -2.7324e+04 \\ 1 & 0 \end{bmatrix} \quad B_{a_{TE}} = \begin{bmatrix} 2.7871e+04 \\ 0 \end{bmatrix}$$

$$C_{a_{TE}} = \begin{bmatrix} -1.8514e+02 & -2.7324e+04 \\ 1 & 0 \\ 0 & 1 \end{bmatrix} \quad D_{a_{TE}} = \begin{bmatrix} 2.7871e+04 \\ 0 \\ 0 \end{bmatrix} \tag{A15}$$

The state space matrices for the upper spoiler actuator are

$$A_{a_{US}} = \begin{bmatrix} -2.7880e+02 & -2.6896e+04 \\ 1 & 0 \end{bmatrix} \quad B_{a_{US}} = \begin{bmatrix} 3.1199e+04 \\ 0 \end{bmatrix}$$

$$C_{a_{US}} = \begin{bmatrix} -2.7880e+02 & -2.6896e+04 \\ 1 & 0 \\ 0 & 1 \end{bmatrix} \quad D_{a_{US}} = \begin{bmatrix} 3.1199e+04 \\ 0 \\ 0 \end{bmatrix} \tag{A16}$$

State Space Matrices for Turbulence Model

The state space form for the turbulence models is

$$\begin{aligned} \dot{x}_g &= A_g x_g + B_g \eta_g \\ \begin{bmatrix} \dot{w}_g \\ w_g \end{bmatrix} &= C_g x_g + D_g \eta_g \end{aligned} \tag{A17}$$

Note that the output of the model consists the acceleration and velocity of the downwash in the freestream flow. Both are needed as input to the BACT equations of motion.

The state space matrices for the wind tunnel turbulence model are

$$A_g = \begin{bmatrix} -2.6322e+02 & -1.7321e+04 \\ 1 & 0 \end{bmatrix} \quad B_g = \begin{bmatrix} 1 \\ 0 \end{bmatrix}$$

$$C_g = \begin{bmatrix} -6.1372e+03 & -7.3026e+05 \\ 4.2160e+01 & 4.9601e+03 \end{bmatrix} \quad D_g = \begin{bmatrix} 4.2160e+01 \\ 0 \end{bmatrix} \tag{A18}$$

The reference speed value for this model is 400 fps because it is close to the experimental test conditions and correlates best with experimental data.

REPORT DOCUMENTATION PAGE

Form Approved OMB No. 0704-0188

1. AGENCY USE ONLY (*Leave blank*)	2. REPORT DATE	3. REPORT TYPE AND DATES COVERED
	June 1998	Technical Publication

4. TITLE AND SUBTITLE
Modeling the Benchmark Active Control Technology Wind-Tunnel Model for Active Control Design Applications

5. FUNDING NUMBERS
522-33-11-01

6. AUTHOR(S)
Martin R. Waszak

7. PERFORMING ORGANIZATION NAME(S) AND ADDRESS(ES)
NASA Langley Research Center
Hampton, VA 23681-2199

8. PERFORMING ORGANIZATION REPORT NUMBER
L-17625

9. SPONSORING/MONITORING AGENCY NAME(S) AND ADDRESS(ES)
National Aeronautics and Space Administration
Washington, DC 20546-0001

10. SPONSORING/MONITORING AGENCY REPORT NUMBER
NASA/TP-1998-206270

11. SUPPLEMENTARY NOTES
Waszak: Langley Research Center, Hampton, VA ; email: m.r.waszak@larc.nasa.gov ; world wide web: http://dcb.larc.nasa.gov

12a. DISTRIBUTION/AVAILABILITY STATEMENT
Unclassified-Unlimited
Subject Category 08 Distribution: Standard
Availability: NASA CASI (301) 621-0390

12b. DISTRIBUTION CODE

13. ABSTRACT (*Maximum 200 words*)

This report describes the formulation of a model of the dynamic behavior of the Benchmark Active Controls Technology (BACT) wind tunnel model for active control design and analysis applications. The model is formed by combining the equations of motion for the BACT wind tunnel model with actuator models and a model of wind tunnel turbulence. The primary focus of this report is the development of the equations of motion from first principles by using Lagrange's equations and the principle of virtual work. A numerical form of the model is generated by making use of parameters obtained from both experiment and analysis. Comparisons between experimental and analytical data obtained from the numerical model show excellent agreement and suggest that simple coefficient-based aerodynamics are sufficient to accurately characterize the aeroelastic response of the BACT wind tunnel model. The equations of motion developed herein have been used to aid in the design and analysis of a number of flutter suppression controllers that have been successfully implemented.

14. SUBJECT TERMS
aeroelasticity, equations of motion, flutter suppression, BACT, Benchmark Models Program, wind-tunnel models

15. NUMBER OF PAGES
32

16. PRICE CODE
A03

17. SECURITY CLASSIFICATION OF REPORT	18. SECURITY CLASSIFICATION OF THIS PAGE	19. SECURITY CLASSIFICATION OF ABSTRACT	20. LIMITATION OF ABSTRACT
Unclassified	Unclassified	Unclassified	